Surface & Coatings Technology 207 (2012) 472–479

Contents lists available at SciVerse ScienceDirect

Surface & Coatings Technology

journal homepage: www.elsevier.com/locate/surfcoat

Tool steel coatings based on niobium carbide and carbonitride compounds

Rafael A. Mesquita [a,b,*], Christopher A. Schuh [a]

[a] Massachusetts Institute of Technology, Department of Materials Science and Engineering, 77 Massachusetts Avenue, Cambridge, MA 02139, USA
[b] University "Nove de Julho", Department of Master Science in Industrial Engineering, Brazil

ARTICLE INFO

Article history:
Received 8 March 2012
Accepted in revised form 16 July 2012
Available online 24 July 2012

Keywords:
Tool steel coatings
NbC
Nb(C,N)
PVD
Bias
Magnetron sputtering

ABSTRACT

Although Physical Vapor Deposition (PVD) is extremely versatile in the palette of coating materials and substrates to which it can be applied, many potentially viable hard coating materials have yet to be explored for deposition on tool steels via PVD processing. Here one family of such coatings is explored: the niobium carbide and carbonitride system. By changing process variables, including bias voltage and working pressure, evaluating the mechanical properties through nanoindentation and correlating the results to microstructural observations by transmission electron microscopy, a preliminary survey of these coating materials and the preferred conditions for their production is presented. Under some conditions of deposition bias and pressure, niobium carbide can be produced with hardness and elastic modulus superior to titanium nitride films, reaching up to 37 GPa and 400 GPa, respectively, for coatings produced under deposition conditions that reduce intrinsic porosity. Nitrogen substitution for carbon leads to intermediate carbonitride compositions with mechanical properties that depend roughly linearly on composition, permitting a degree of tunability of the coating properties.

1. Introduction

Since the 1960s, hard coatings have been applied to reduce wear and improve friction characteristics of tool steels, especially in, e.g., cutting tools [1]. Due to its high hardness, one of the first compounds used in such applications was titanium carbide. TiC was first applied by Chemical Vapor Deposition, CVD [2,3], although the high temperature of this process proved unsuitable for many steel substrates, restricting its application mainly to solid carbide tools. Physical Vapor Deposition (PVD) was developed as an effective way to reduce the processing temperature to less than 550 °C, enabling coatings on high alloy steels [4–6]. In the PVD chamber, nitriding reactions are induced more easily than are carburizing reactions, so nitrides gradually replaced carbides, with titanium nitride (TiN) being the most widely used compound [7] due to its similarity to TiC. Today PVD TiN compounds are often modified with Al to increase thermal stability [7]. In fact, due to the large number of studies on TiN or TiAlN coatings and their extensive use in industry for tool steels applied to cutting or forming tools [8], these compounds are used as a baseline reference for the results of the present paper.

As a result of the above trend, most of the literature on PVD coatings over tool steels is directed at the study of nitrides, with the number of studies on carbides being much smaller. However, based on the requirements of hard coatings (high strength and thermal stability) [9], there are a number of carbide systems that seem potentially suitable even though they have not been widely studied as yet. Examples of specific interest to the present work are niobium carbide and niobium carbonitride. NbC seems a natural candidate hard coating material, since as a bulk compound it exhibits a hardness beyond 20 GPa and a melting point above 3000 °C [10]. NbN exhibits full mutual solubility in NbC [11], so a wide range of carbonitride materials could also be fashioned within this family. This could permit, e.g., tuning of toughness, thermal expansion coefficient and other secondary properties needed for high performance applications.

Despite these generally positive expectations for NbC and NbCN as potential coating materials, to the authors' knowledge there are no systematic reports in the literature on the effect of processing parameters upon even the most basic of mechanical properties of such materials produced by sputtering PVD, such as, e.g., hardness and elastic modulus. One report in this sense is on vacuum cathode arc deposition of NbC [12], showing exceptional properties, with hardness values above 40 GPa. For mechanical properties of sputtered NbC coatings, only one reference was found [13], but the hardness values obtained were below 25 GPa, which is below the hardness of traditional TiN sputtered coatings (~30 GPa) applied to tool steels; we are also not aware of published results on the mechanical properties of niobium carbonitride coatings applied specifically to tool steels.

The purpose of the present paper is therefore to present a study on the fabrication, mechanical properties and microstructure of niobium carbide and carbonitride coatings on H13 hot work tool steel, produced by PVD using direct sputtering of NbC and reactive sputtering with N_2 atmospheres. Beginning with studies on binary NbC, traditional PVD variables such as the deposition pressure and bias are changed to

* Corresponding author at: Av. Francisco Matarazzo, 612, São Paulo, SP, 05001-100, Brazil. Tel.: +55 11 3665 9355; fax: +55 11 3665 9325.
E-mail address: rafael.mesquita@uninove.br (R.A. Mesquita).

0257-8972/$ – see front matter
http://dx.doi.org/10.1016/j.surfcoat.2012.07.052

evaluate their effect on hardness and microstructure. Subsequently, nitrogen is introduced and nitrogen content is used to tailor the coating structure and properties. For the preferred conditions, we identify coatings with hardness and elastic modulus values either similar to or higher than those of conventional TiN. By using transmission electron microscopy, these properties are correlated to the films' microstructure.

2. Experimental details

PVD films were produced by magnetron sputtering, in a system from AJA International (ATC 2000 UHV), with balanced design. This system operates via co-sputtering with up to 6 targets, with 2 targets being used in the present paper: NbC, sputtered under radio frequency (RF) conditions due to its non-conductive and brittle behavior, and metallic Nb, sputtered with direct current (DC). The targets, of 50.4 mm diameter, are placed with a focusing arrangement, with the substrates located at the focal point and rotating at 15 rpm. The distance from target to substrate was maintained at approximately 200 mm.

A base pressure of less than 3.10^{-5} Pa (2.10^{-7} Torr) and working pressures of 0.40 Pa and 0.67 Pa (3 and 5 mTorr) were employed; throughout the text, working pressure refers to the total pressure in the chamber. Ar was the main process gas, but N_2 was also used for the carbonitride compositions. The system substrate bias was varied between 0 and 150 V. All depositions were conducted using a 400 °C substrate temperature, as measured by a k-type thermocouple in contact with the sample holder; temperature was constant throughout the process, with variation of less than 0.5 °C.

Direct sputtering from a NbC target (99.5% pure) was used for both the NbC and NbCN coatings, with the N additions effected by sputtering under a N_2-rich atmosphere, with the following conditions: NbC sputtering under 0.08 Pa N_2 partial pressure (20% of total pressure) and simultaneous sputtering of NbC and metallic Nb (99.9% pure) targets, under the same N_2 atmosphere. For the NbN, traditional reactive Nb sputtering under N_2 was used, with 0.07 Pa partial pressure of N_2. The details for all conditions are given in Table 1. Before sputtering, substrates were polished down to 1 μm with diamond media, leading to Ra roughness of about 0.02 mm. Before sputtering, samples were cleaned in acetone, dried with nitrogen and plasma cleaned using 25 W and 150 V bias for 10 min. Due to the low deposition rate (of about 100 nm/h), the sputtering time was between 4 and 5 h for each condition. This slower deposition process is related to the confocal arrangement and also to the small target diameter and sputtering power. However, it is important to mention that the AES results showed no important contaminants, such as oxygen or other gases, during such long deposition times. After sputtering, the thickness of all coatings was measured to be around 400 nm, the only notable exception being the 0 V bias NbC film with a thickness of about 700 nm.

All films were deposited on glass and on H13 tool steel substrates. The tool steel samples were heat treated before deposition, through hardening at 1020 °C and double tempering at 600 °C for 2 h each, leading to a hardness of 45 HRC. This procedure is common for hot work tool steels [13], and leads to a stable dispersion of secondary hardening carbides that only show extensive coarsening and hardness loss at temperatures above 600 °C [14].

Mechanical properties were characterized by nanoindentation, using a Hysitron nanoindenter with a Berkovich tip. The same tip was used for all experiments, with an area function carefully calibrated for indentation depths between 20 and 80 nm; the error in relation to the fused silica calibration standard was below 5% in terms of hardness and modulus, as can be observed in Fig. 1. These low indentation depths were used to preserve the accuracy of hardness and modulus measurements, as the thickness of the coatings varied between 300 and 600 nm. Therefore, indentation depths between 30 and 50 nm were used in all experiments to ensure a bulk measurement free of interference from the substrate. The indentation load was adjusted (between 600 and 3000 μN) to achieve these depths depending upon the coating hardness. The same nanoindenter was used to determine surface roughness in scanning contact-imaging mode.

Phase characterization was performed initially by X-ray diffraction (XRD) using a Rigaku H3R Cu-source Powder Diffractometer, operating at 50 kV and 200 mA with Cu Kα radiation. A scatter slit and divergence slit of 0.5° were used to concentrate the diffraction beam on the small samples (about 1 cm^2) and to increase the signal/noise ratio respectively. All patterns were then analyzed using Rietveld refinement, leading to precision on lattice parameters (a) better than 0.0005 nm. This accuracy level was obtained by the use of an external standard Si powder sample and also by the use of substrate iron peaks as an internal standard. Differences in lattice parameter (Δa) were used to calculate the residual elastic macro strain via Hooke's law for a state of plane stress: $\sigma = -E \cdot \varepsilon/(2\upsilon)$, where E is the Young's modulus, $\varepsilon = \Delta a/a_0$ the residual strain calculated with respect to the lattice parameter of NbC, $a_0 = 0.447$ nm [15,16], and $\upsilon = 0.235$ [17] the Poisson ratio for NbC. This method was preferred to the sine-square psi traditional XRD method, due to the low intensity in high angle reflections and considerable broadening observed in many of the conditions. The method has been previously validated for coatings [18] when the stress-free compound lattice parameter is known and the sample lattice constant is determined with high accuracy. In the present case, both conditions were satisfied, with the lattice constant for NbC calculated from sources of high quality with variation between them less than 0.00006 nm [15,16].

The XRD data were also used to estimate the C to N ratio in Nb(C,N) films based on the lattice parameter (determined by Rietveld refinement) and Vegard's law, with an apparent accuracy better than 0.001 nm. The Vegard reference relationship for this calculation is based on patterns of high quality for the pure NbC [15,16] and NbN [19–21] compounds and three indexed patterns for intermediary $NbC_{0.5}N_{0.5}$ (average of literature determinations [22,23]). We note that most of the available powder diffraction files for NbN represent a stoichiometry of $NbN_{0.9}$, but here the ideal 1:1 ratio was assumed. This indirect, structural means of determining N content was also augmented with results from Auger Electron Spectroscopy (AES), Physical Electronics Model 700 Scanning Auger Nanoprobe (LS). The N content calculated by XRD and AES was in agreement, as presented in Table 1.

The results of hardness and residual stresses were correlated to sample surface topography by analyzing the as-coated surfaces under a field emission scanning electron microscope (SEM), Zeiss Nvision 40. This apparatus has also a focused ion beam (FIB) source, with Ga+

Table 1
Conditions used to produce the various compositions of $NbC_{(1-x)}N_x$ coatings. The errors for both methods of nitrogen content determination are around 15% of measured values, calculated from the Rietveld error on the lattice parameter determination or by the AES analysis uncertainty.

Designation	Sputtering conditions (targets, power, time)	N partial pressure (Pa)	x calculated by XRD	x measured by AES	Bias and total pressure
NbC	NbC: RF 200 W, 5 h	–	–	–	Low: 0 V, 0.40 Pa High: 70 V, 0.67 Pa
$NbC_{0.6}N_{0.4}$	NbC: RF 200 W, 3 h	0.08	0.40	0.35	Low: 0 V, 0.40 Pa High: 70 V, 0.67 Pa
$NbC_{0.4}N_{0.6}$	NbC: RF 200 W, 3 h Nb: DC 250 W, 3 h	0.08	0.61	0.56	Low: 0 V, 0.40 Pa
NbN	Nb: DC 250 W, 1 h	0.07	–	–	Low: 0 V, 0.40 Pa High: 150 V, 0.40 Pa

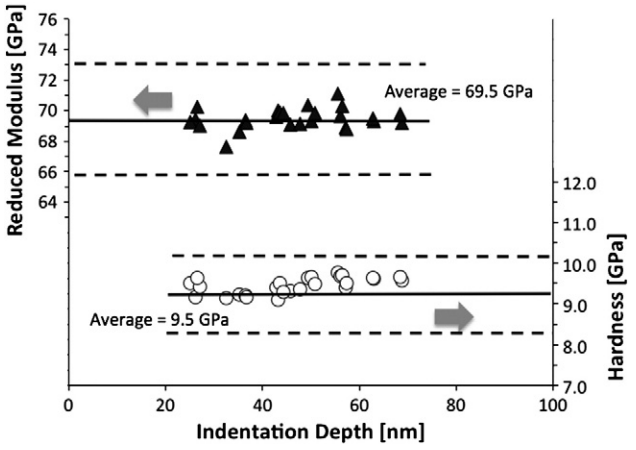

Fig. 1. Comparison of data from shallow depth indentation on fused silica, over a depth range matching that used for the Nb(C,N) coatings, due to the their reduced thickness. The standard silica sample presents a reduced modulus of 69.5 ± 3.5 GPa and hardness of 9.5 ± 0.5 GPa.

ions, that was used to extract samples for transmission electron microscopy (TEM) evaluations with a JEOL 200 kV instrument. FIB preparation involved cutting samples from the coating using 1.5 nA and 30 kV conditions, initial thinning at 30 kV and 80 pA to a thickness of 300 nm, slow thinning at 30 kV and 40 pA to a thickness of 150 nm, and final thinning using low acceleration conditions of 5 kV and 20 pA. The final thickness of the TEM samples was between about 60 and 100 nm in the imaged regions. FIB trenches were also used to determine the thickness of deposited coatings on the steel substrates.

3. Results

3.1. NbC coatings

The sputtering conditions were found to dramatically affect the properties and surface conditions of the sputtered NbC coatings. This was initially recognized by comparing the coating thicknesses and visual surface appearances, as shown in Fig. 2. The increase in bias resulted in an apparently linear decrease of thickness (Fig. 2a) and also led to loss of coating soundness (Fig. 2b). Fragmentation of the deposited films could be observed visually as shown in Fig. 2b, where the images show films deposited on glass slides and analyzed by a transmission optical microscope under low magnification. The white spots are locations where light was transmitted, and thus represent delaminated regions of the coating. This effect was largely suppressed in the low bias condition (0 to 70 V), but was quite strong in the high bias condition (150 V). Therefore, X-ray diffraction could not be properly conducted on the 150 V bias sample, as most of the coating detached from the surface during preparation.

On the other hand, bias positively affected the hardness and Young's modulus, as shown in Fig. 3. We found that a small increase in the total deposition pressure was also important to mechanical properties, and thus one condition for high pressure is presented separately in Fig. 3. While the 0 V bias condition rendered NbC coatings with hardness and modulus below the values expected for bulk samples (about 22 GPa and 400 GPa, respectively [9]), a strong increase in both properties is observed with bias. Most interestingly, the hardness values at biases above about 70 V are well above the nominal bulk NbC hardness, reaching values as high as 32 GPa, and even further to 37 GPa for the increased deposition pressure.

The XRD results (Fig. 4) suggest that all of the tested processing conditions led to the deposition of NaCl cubic NbC (δ phase).There is a large range of homogeneity of δ phase in NbC_x, with x ranging from 0.8 to 1.0, from a defect mechanism with vacancies occurring on the C sublattice [24]. Such changes lead to a decrease in lattice parameter of about 0.004 nm, when x varies from 1.0 to 0.8. The measured lattice parameter for our pure NbC, sputtered at 0 V bias, is 0.4482 nm, which is very close to the expected lattice parameter for NbC of 0.4469 nm [15,16]. The Auger results also point to an atomic concentration of 50 at.%. Therefore, the coating was assumed to be close to x = 1; the small differences in lattice parameter are mostly likely related to residual stresses, although these are expected to be small in the 0 V bias condition due to the porous microstructure, as will be discussed shortly. A possible excess of amorphous carbon was not observed, but could be possible in these systems, according to Ref. [13].

Small shifts in the peak positions to smaller diffraction angles were observed when bias or working pressure was increased. This indicates an increase in the lattice parameter in the direction normal to the coating surface, which is related to compressive biaxial stresses in the plane. These shifts were converted to residual stress values as shown in Fig. 5. A roughly linear relation is observed in terms of the increase in both the

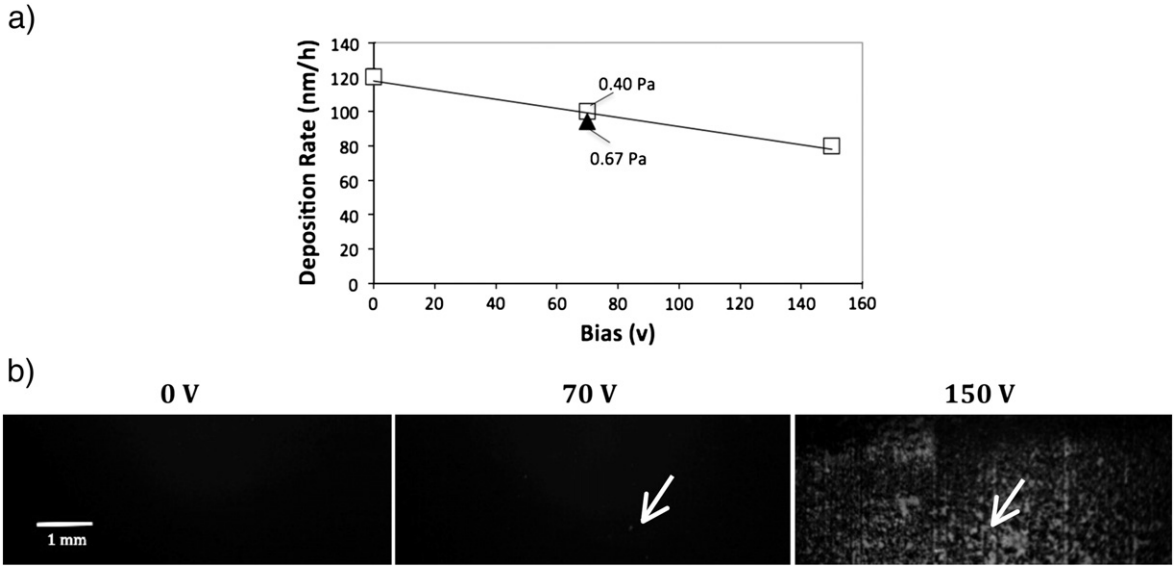

Fig. 2. Variation in deposition rate (a) and soundness of the deposited film (b) with the bias condition. No significant changes were noticed with the variation of working pressure from 0.40 to 0.67 Pa. In (b) films deposited on glass were compared; the light areas refer to where the microscope light is transmitted, indicating an absence of coating and thus damage (as noted by the arrows).

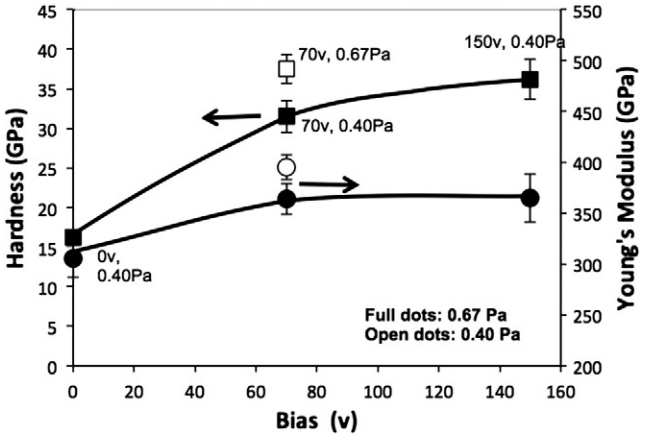

Fig. 3. Data for mechanical properties, in terms of sputtering conditions of bias and total pressure. Data was plotted according to an empirical relation, depending on the product of bias and pressure. The open points relate to the coatings sputtered with higher pressure (0.67 Pa, at 70 V), and the solid points with lower pressure (0.40 Pa), with bias values of 0 V, 70 V and 150 V.

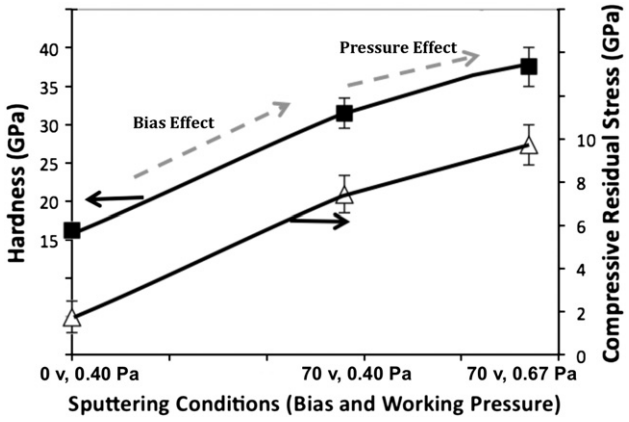

Fig. 5. Hardness and compressive residual stress for NbC, plotted as a function of the deposition bias, for two different working pressures.

hardness and residual stresses as the bias or working pressure is increased. It is certainly striking that these two mechanical measurements appear to follow identical trends with the processing parameters; this is an issue that we will return to in the discussion.

Fig. 5 also contains some annotation that better illustrates the effects of increasing the working pressure. From the limited data available, it appears that pressure has a significant but decidedly secondary influence. An increase in pressure results in about 20% increase in hardness, whereas about double the hardness is obtained upon changing the bias from zero to 70 V.

In addition to the macro residual stress that causes peak shifts, peak broadening is also observed for samples produced with different bias conditions. By applying Rietveld refinement and the Williamson–Hall plot for the full width at half maximum data, the broadening was shown to be related only to the increase in microstrain between the conditions of 0 V bias and 70 V bias. The microstructure observations, shown later, confirm this point, as no grain size change was observed among these various samples.

In addition to changes in hardness, modulus and residual stress, the processing conditions of the coating also affect the surface roughness, which dramatically decreases from zero to 70 V bias. This is shown in Fig. 6(a) and (b). Further change to the surface morphology is also induced by increasing pressure from 0.40 to 0.67 Pa, as shown in Fig. 6(b) and (c).

All of the above results can be appreciated in the context of the coating microstructure by observing the bright-field TEM images in Fig. 7, showing cross-sections of binary NbC coatings, for low and high bias conditions. Again, a dramatic change is observed with the application of bias, and this change pertains to apparent porosity in the coatings.

First, in the low bias condition in Fig. 7a, we observe a very fine polycrystalline structure. Several bright areas were observed in the

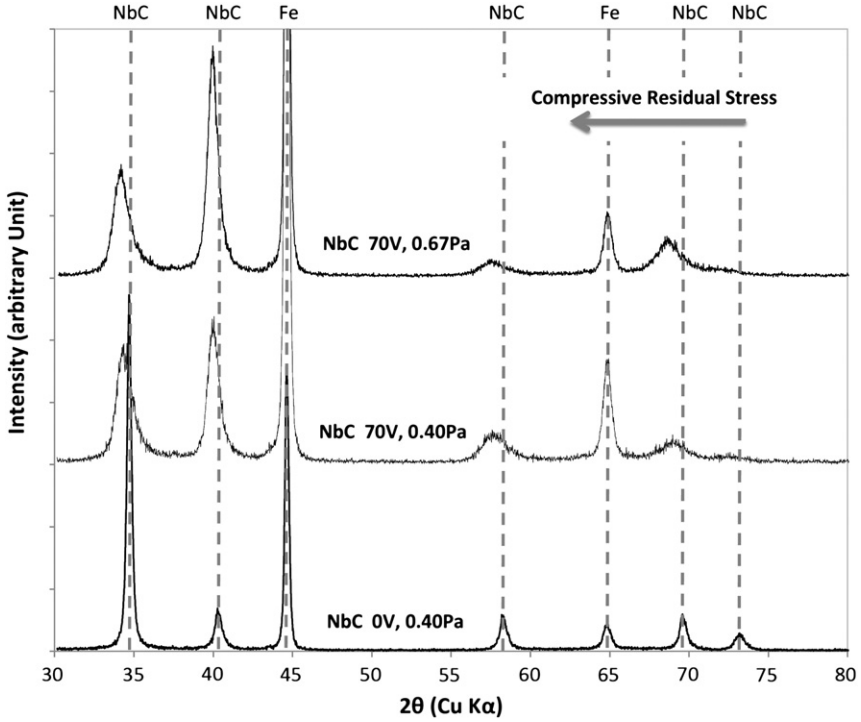

Fig. 4. X-ray data showing the single phase cubic carbide and also the peak shift to lower diffraction angles due to compressive residual stress (see also Fig. 4). Films deposited on steel substrates.

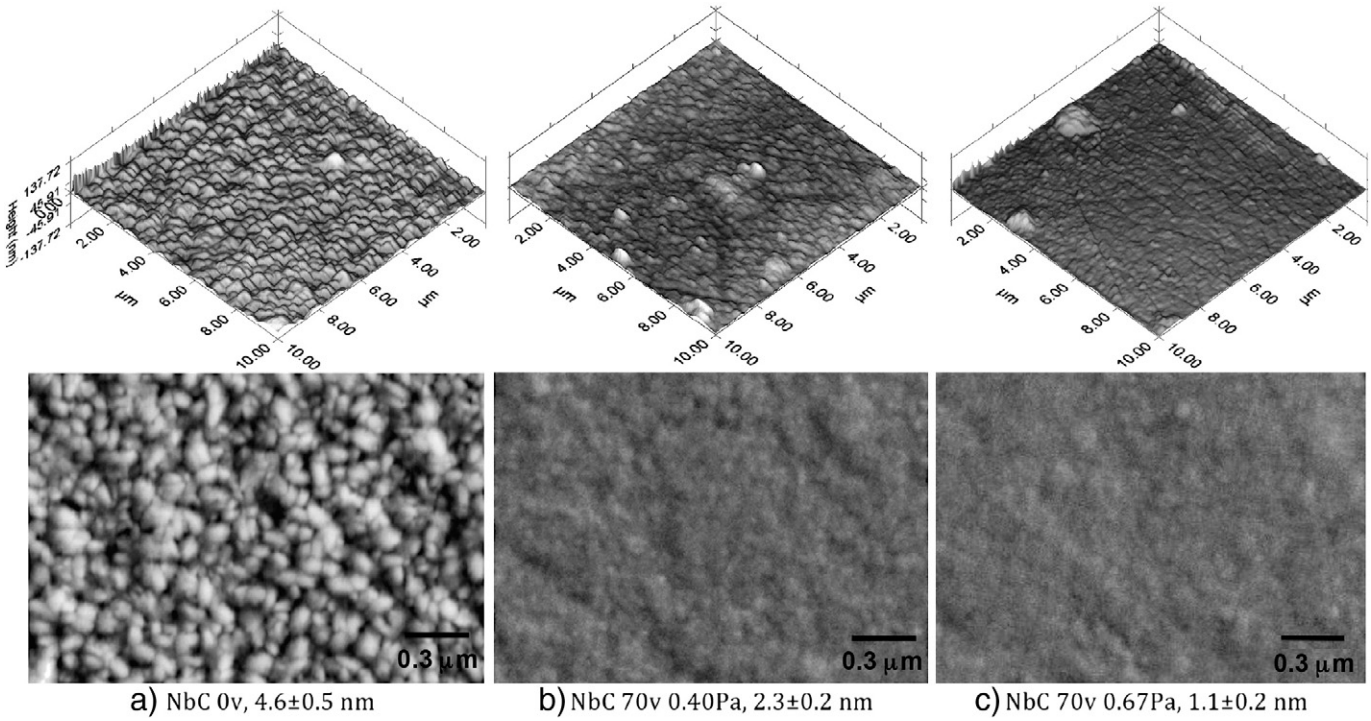

Fig. 6. Surface roughness of NbC for each sputtering condition: (a) zero bias, (b) 70 V bias and 0.40 Pa total pressure, (c) 70 V bias and 0.67 Pa total pressure. Images were obtained by scanning probe microscopy (top images) and scanning electron microscopy (bottom images). The roughness values refer to the root-mean-square roughness.

low bias sample, in practically all of the examined film sections; a few typical examples are shown in Fig. 7a, marked by white arrows. Extensive evaluations of these samples, using dark and bright fields as well as different FIB preparation conditions (of which one example is shown in Fig. 8), led us to the conclusion that these bright regions are in fact porosity, small voids located between the grains of the columnar structure. Some relatively larger voids (with characteristic lengths of about 2 nm) as well as more typical smaller regions (less than 1 nm in size) were observed. Such nanoporosity has been observed both in experiments on low bias PVD TiN samples [25] and in kinetic Monte Carlo simulations of thin film growth [26,27]. Compared to the studies on TiN in Ref. [25], the results in Fig. 7a indicate a somewhat higher level of porosity in the present films.

On the other hand, samples prepared at higher process intensities do not exhibit these regions of porosity, and in general seem much more dense (Fig. 7b). In addition, these samples also tend to exhibit more contrast arising from lattice defects. This is consistent with the XRD results that indicated a significant increase in microstrain with increasing bias.

3.2. Nb(C,N) coatings

Fig. 9 presents the XRD diffractograms for all of the carbide, nitride, and carbonitride compositions produced without bias. These all show the typical pattern for the face-centered cubic phases, with the NbC and NbN peaks separated from each other by a small but important difference, and the intermediate compositions positioned between the two pure compounds as expected for solid solutions. The 70 V bias samples exhibited some peak shift due to residual stress.

The mechanical properties of these films are shown in Fig. 10. A linear, rule-of-mixture-like trend is observed with respect to nitrogen content for all of the films, including those produced under high bias conditions. The nitride phase is considerably more compliant and weaker than the carbide one, and in between it is possible to finely tune the coating to different levels of hardness and stiffness by adjusting the nitrogen content. And, as reported above for the NbC phase, higher processing bias in every case leads to higher hardness and stiffness, presumably because of an increase in density (cf. Fig. 7). Indeed, our TEM observations on the low bias specimens containing N also show porosity in similar levels to the low-bias NbC films (see Fig. 8). The nitride and carbonitride films also exhibit essentially the same columnar grain structure, with a characteristic grain width of about 30 nm (Fig. 11).

4. Discussion

4.1. Process variables and properties of NbC coatings

The above results show that using PVD, NbC coatings with hardnesses at the same level or even slightly higher than more traditional PVD coatings can be produced. More specifically, with hardness values up to 37 GPa, the present coatings are reasonably matched to TiN (23 GPa), (Ti,Al)N (30 GPa) or CrN (23 GPa), according to typical industrial values [28]. These mechanical property values are not, however, attained at all processing conditions, and here we find that they are induced by the increase in bias condition, and are accompanied by considerable increase of compressive residual stresses.

This effect of bias is well-known for other PVD coatings, and is appreciated as yielding more densification and higher compressive residual stresses. For example, these trends have been reported in TiN films produced by PVD [29] or CrN [30]. In fact, similar trends have been reported for NbC coatings produced by arc evaporation [11]. Based on our observations in Fig. 7, it seems likely that at least in the present case, the improvement in mechanical properties may be attributed to the elimination of nanoporosity in these films. As shown by the traditional Thorthon structure zone model [31], a low ratio of substrate to melting temperature of the coated compound (Ts/Tm) leads to films of Type I morphology, which are less dense and have compromised mechanical properties. The sensitivity of NbC to this effect is expected to be considerably higher than for nitrides such as TiN or CrN, due to the higher melting point of NbC, which is about 3800 K, vs. 3200 K for TiN and 1800 K for CrN.

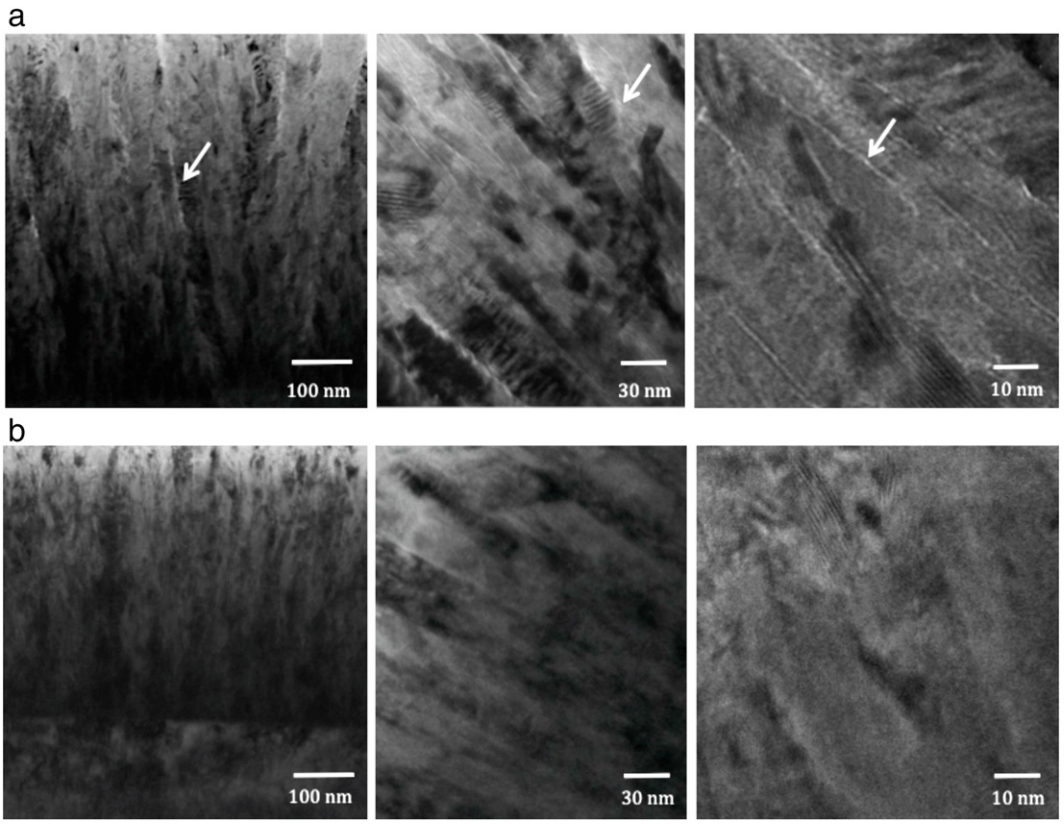

Fig. 7. TEM micrographs of NbC sputtered under: (a) zero volt bias and (b) high bias conditions (70 V). Bright areas where the beam was transmitted are interpreted as porous regions.

On the other hand, upon eliminating the porosity by increasing the bias, as shown in Fig. 7, both the hardness and elastic modulus increase to values consistent with expectations for the bulk compound (Fig. 3). This change in properties is also accompanied by a continuous increase in residual stress, which seems to achieve levels higher than are common for nitrides. Nevertheless, the comparison of residual stress between NbC and TiN or other coatings is less direct than the comparison of hardness, due to the difference in elastic moduli; the modulus of NbC is higher by a factor of almost two than that of TiN, which means that at the same strain level the residual stress in NbC is inflated by the same factor. The coatings may best be compared on the basis of residual strain. Literature results for TiN coatings show stresses between 3 and 8 GPa [32–35] for bias of about 70 to 100 V, which relates to strain between 1.0 and 2.0%. This strain level is similar to that determined for the present NbC coatings, about 1.0% for 70 V bias. There are many reasons for this observed increase in compressive residual elastic strain (and thus residual stress) upon increasing the bias, two of which are considered the most important [7,8,26]: i) thermal effects related to the different thermal expansion between substrate and coating, and ii) the introduction of strain during sputtering. All these effects cause an increase in densification, and thus are consistent with the observed increase in residual stresses.

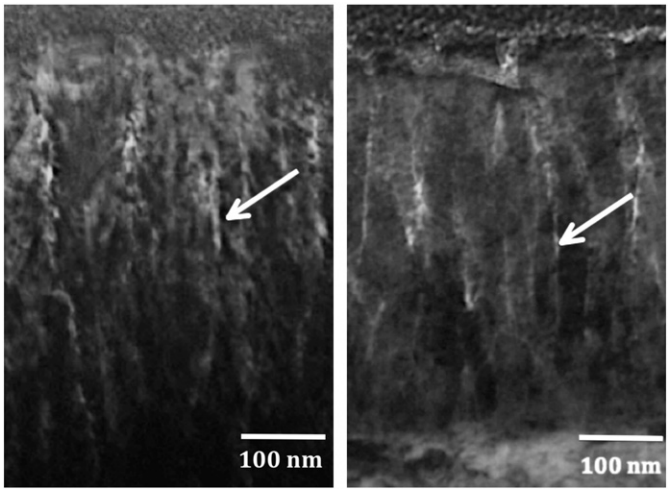

Fig. 8. Zero bias NbC (left image) and $NbC_{0.60}N_{0.40}$ (right image) microstructures, evaluated in thicker TEM lamellas (about 100 nm).

On the other hand, the highest bias conditions used in the present paper, especially 150 V, show that the deposited film is not sound and was almost fully delaminated from the surface. Extreme values of compressive stresses, about 10 GPa, are expected for such conditions, and these are likely the main limitation against continuously increasing the applied bias. For example, the literature suggests that residual stresses over 7 GPa in TiN also tend to cause film deterioration [35–37]. In terms of physical mechanisms associated with the change in bias, many reports in the literature for other compounds [36–40] suggest that the stronger acceleration of the positive ions against the substrate leads to denser films. Our results are generally consistent with this explanation, as shown in Figs. 3 and 7. The result for the increased bias voltage would then be related to a higher kinetic energy of the arriving Ar ions. On the other hand, the increase in pressure is related to a larger number of impinging ions. This role of bombardment conditions is in agreement with previous models in literature, which consider the average energy delivered per atom and the flux of atoms [40–43].

Another fact related to the PVD processing variables that is worth discussing relates to the final surface roughness (Fig. 6). The higher degree of smoothness on the surface of high bias samples may be explained by a constant "plasma cleaning" during the deposition process by Ar^+ ions accelerated against the surface. It is reasonable that this roughness would be affected by both bias and working pressure,

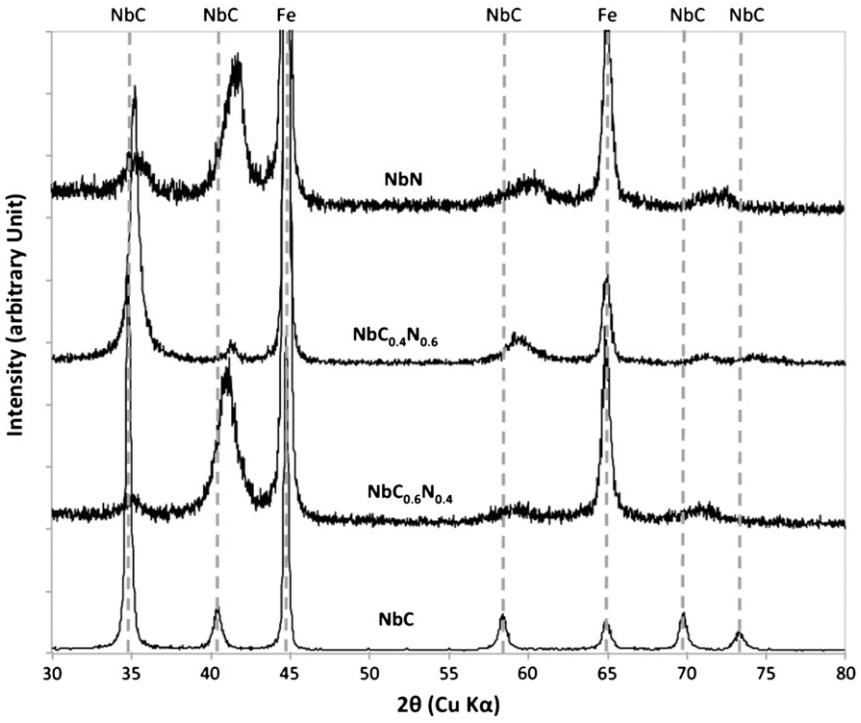

Fig. 9. Untreated data from X-ray diffraction, for all studied compositions deposited on steel. Only the zero bias samples were employed in this analysis, because the high bias samples present strong peak shift due to residual stresses. The difference in signal/noise of patterns is mainly caused by the higher thickness of the NbC coatings as well as possible differences in preferential orientation. All films are deposited on steel substrates.

because, as discussed, they would control the speed and number of shocking atoms, respectively.

Therefore, the effects of bias and change in working pressure seem consistent with the same mechanisms proposed for traditional PVD coatings. Some of these effects are stronger for NbC than for other compounds due to the lower homologous processing temperature Ts/Tm, which in turn is caused by the high melting point of NbC.

4.2. Effect of nitrogen in NbC PVD coatings

As shown in Figs. 8 to 10, the differences in structure and mechanical properties tend to vary linearly with N substitution for C in NbC. The hardness differences in the intermediate compositions of the system $NbC_{(1-x)}N_x$ can be attributed to the partial substitution of Nb–C bonds with Nb–N bonds, which naturally leads to a lower hardness relative to the bulk hardness of NbC (about 22 GPa), and can approach that of NbN (about 14 GPa) [9]. Nevertheless, the hardness of $NbC_{0.6}N_{0.4}$ is still about 28 GPa, which is in line with the common range for TiN coatings widely used in industry [7,27]. Other physical properties can be expected to exhibit similar behavioral trends in the mixed Nb(C,N) composition range, e.g. N can be used to increase the thermal expansion coefficient relative to NbC [9], which in turn could lead to better compatibility characteristics when coating metallic substrates such as the tool steels evaluated here [8].

Therefore, the findings from the present paper show that N additions may be used to control the hardness and modulus of NbC direct sputtered PVD coatings. We suggest that this may in fact be a preferred coating than a simple binary NbC produced with the same hardness and modulus by lowering the applied bias; the N-bearing coatings can achieve the same suite of properties without introducing porosity, which may also

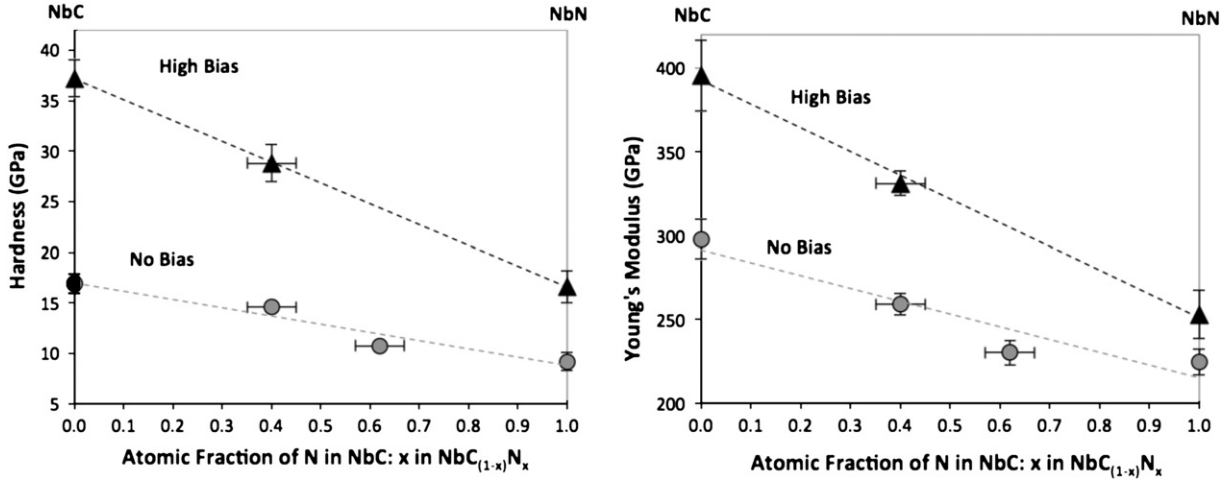

Fig. 10. Mechanical properties of the coatings as a function of the nitrogen content calculated according to Fig. 1, for the zero bias condition.

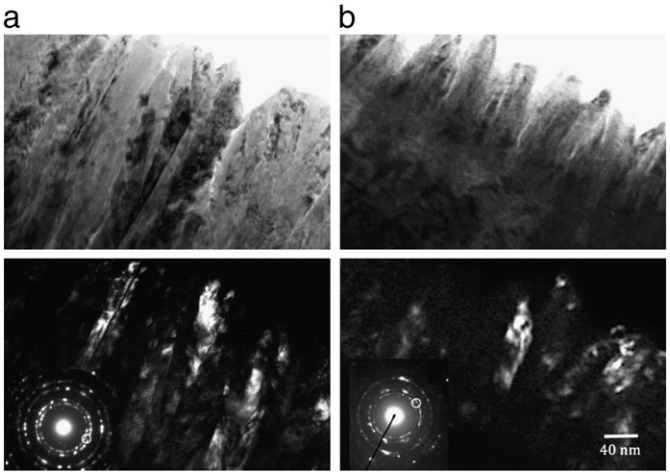

Fig. 11. Microstructure of the PVD films of (a) NbC and (b) and $NbC_{0.6}N_{0.4}$, both sputtered without bias. The bright and dark field images illustrate a similar columnar grain structure for both compositions. Part of the substrate is present in the bright field image of (b).

be expected to have secondary undesirable effects. These include lower toughness, reduced corrosion protection, decohesion, etc. This hardness control may be important to applications where lower strength is acceptable given that better toughness is required, such as those with failure mechanisms related to coating chipping or spalling.

5. Conclusions

Processing conditions for the production and microstructural design of niobium carbide and carbonitride PVD coatings, via magnetron sputtering, were evaluated experimentally in this paper, for deposition on tool steel samples. The most salient findings are presented below:

- The microstructure, properties and surface hardness of Nb-based hard coatings are shown to be very dependent on the bias increase, but also influenced by the working pressure. These dependencies are stronger than are observed for TiN or CrN.
- One of the microstructural explanations for the effect of bias upon mechanical properties is related to a strong change in nanoporosity, which is quite high in the low bias samples and apparently absent after sputtering under high bias conditions. This observation is generally in line with traditional models for the bias effect, with the notable caveat that NbC has a higher sensitivity to this effect because of its higher meting temperature, in relation to nitrides.
- On the other hand, very high values of bias, such as 150 V, tend to cause the deterioration of the film via delamination and flaking. This is probably a result of the extremely high levels of compressive residual stresses developed under the highest bias conditions.
- Using optimized sputtering conditions, NbC hard coatings can thus be produced with dense microstructures, leading to hardness values higher than those reported for traditional nitrides, such as TiN. Hardnesses as great as 37 GPa and elastic moduli as high as 400 GPa are reported here.
- At the same time, to produce films with hardness and physical properties closer to traditional TiN films, N modification to NbC is a viable approach. The carbonitride coatings have the same crystal structure and similar microstructure, but exhibit linear rule-of-mixture-like behavior between the harder carbide phase and the softer and more compliant nitride phase.

Acknowledgments

R.A. Mesquita thanks FAPESP for supporting the research conducted at MIT. Financial support by the Companhia Brasileira de Metalurgia e Mineração (CBMM) is also gratefully acknowledged. The authors also thank Dr. Hun Kee Lee (MIT), for his help in the obtaining of high-accuracy nanoindentation results.

References

[1] W. Schintlmeister, W. Wallgram, J. Kanz, K. Gigl, Wear 100 (1984) 153.
[2] H.E. Hintermann, Wear 47 (1978) 407.
[3] T. Takahashi, K. Sugiyama, K. Tomita, J. Electrochem. Soc. 114 (1967) 1231.
[4] W.D. Sproul, R. Rothstein, Thin Solid Films 126 (1985) 257.
[5] W. Schintlmeister, W. Wallgram, J. Kanz, Thin Solid Films 107 (1983) 117.
[6] W.D. Münz, D. Hofmann, K. Hartig, Thin Solid Films 96 (1982) 79.
[7] S. PalDey, S.C. Deevi, Mater. Sci. Eng., A 342 (2003) 58.
[8] G. Roberts, G. Krauss, R. Kennedy, in: Tool Steels, 5th ed., ASM International, Materials Park, OH, 1998, p. 220, (pp. 313–323).
[9] B.M. Kramer, Thin Solid Films 108 (1983) 117.
[10] C. Subramanian, K.N. Stratford, T.P. Wilks, L.P. Ward, J. Mater. Process. Technol. 56 (1996) 385.
[11] Foreign Technology, Met. Sci. Heat Treat. 4 (1962) 210.
[12] A. Bendavid, P.J. Martin, T.J. Kinder, E.W. Preston, Surf. Coat. Technol. 163/164 (2003) 347.
[13] N. Nedfors, O. Tengstrand, E. Lewin, A. Furlan, P. Eklund, L. Hultman, U. Jansson, Surf. Coat. Technol. 206 (2011) 354.
[14] R.A. Mesquita, C.A. Barbosa, E.V. Morales, H.-J. Kestenbach, Metall. Mater. Trans. A 42 (2011) 461.
[15] W. Wong-Ng, H. McMurdie, B. Paretzkin, C. Hubbard, A. Dragoo, Powder Diffr. 3 (1988) 55.
[16] G. Will, R. Platzbecker, Z. Anorg. Allg. Chem. 627 (2001) 2207.
[17] A. Nino, A. Tanaka, S. Sugiyama, H. Taimatsu, Mater. Trans. 51 (2010) 1621.
[18] M.A. Moram, Z.H. Barber, C.J. Humphreys, T.B. Joyce, P.R. Chalker, J. Appl. Phys. 100 (2006) 023514.
[19] A.N. Christensen, Acta Chem. Scand. A 31 (1977) 77.
[20] A.N. Christensen, Acta Chem. Scand. A 32 (1978) 89.
[21] G. Heger, O. Baumgartner, J. Phys. C: Solid State Phys. 13 (1980) 5833.
[22] N. Pessall, R.E. Gold, H.A. Johansen, J. Phys. Chem. Solids 29 (1968) 19.
[23] H. Bittner, H. Goretzki, F. Benesovsky, H. Nowotny, Monatsh. Chem. 94 (1963) 518.
[24] J.F. Smith, O.N. Carlson, J. Nucl. Mater. 148 (1987) 1.
[25] I. Petrov, L. Hultman, U. Helmersson, J.-E. Sundgreen, Thin Solid Films 169 (1989) 299.
[26] I. Petrov, P.B. Barna, L. Hultman, J.E. Greene, J. Vac. Sci. Technol. A 21 (2003) S117.
[27] S. Ruan, C.A. Schuh, J. Appl. Phys. 107 (2010) 073512.
[28] M. Van Stappen, L.M. Stals, M. Kerkhofs, C. Quaeyhaegens, Surf. Coat. Technol. 74 (75) (1995) 629.
[29] W.D. Sproul, P.J. Rudni, M.E. Graham, Surf. Coat. Technol. 39/40 (1989) 355.
[30] T. Hurkmans, D.B. Lewis, H. Paritong, J.S. Brooks, W.D. Münz, Surf. Coat. Technol. 114 (1999) 82.
[31] J.A. Thornton, Annu. Rev. Mater. Sci. 7 (1977) 239.
[32] M. Benegra, D.G. Lamas, M.E.F. de Rapp, N. Mingolo, A.O. Kunrath, R.M. Souza, Thin Solid Films 494 (2006) 146.
[33] R. Machunze, G.C.A.M. Janssen, Thin Solid Films 517 (2009) 5888.
[34] A.G. Gómez, A.A.C. Recco, N.B. Lima, L.G. Martinez, A.P. Tschiptschin, R.M. Souza, Surf. Coat. Technol. 204 (2010) 3228.
[35] N.J.M. Carvalho, E. Zoestbergen, B.J. Kooi, J.Th.M. De Hosson, Thin Solid Films 429 (2003) 179.
[36] A.J. Detor, A.M. Hodge, E. Chason, Y. Wang, H. Xu, M. Conyers, A. Nikroo, A. Hamza, Acta Mater. 57 (2009) 2055.
[37] D. Bhaduri, A. Ghosh, S. Gangopadhyay, S. Paul, Surf. Coat. Technol. 204 (2010) 3684.
[38] P.H. Mayrhofer, C. Mitterer, L. Hultman, H. Clemens, Prog. Mater. Sci. 51 (2006) 1032.
[39] K.-H. Müller, J. Appl. Phys. 62 (1987) 1796.
[40] I. Petrov, F. Adibi, J.E. Greene, L. Hultman, J.-E. Sundgren, Appl. Phys. Lett. 63 (1993) 36.
[41] C.A. Davis, Thin Solid Films 226 (1993) 30.
[42] S.M. Rossnagel, J.J. Cuomo, Thin Solid Films 171 (1989) 143.
[43] H. Windischmann, Crit. Rev. Solid State Mater. Sci. 17 (1992) 547.